International Journal of Technology

http://ijtech.eng.ui.ac.id



Research Article

Validation of a Temporary External Fixator for Mandibular Reconstruction: A Biomechanical and Finite Element Analysis

Rungsan Chaiyachet¹, Weerayut jina¹, Ekkachai Kanchanatip², Teerawat Paipongna³, Surasith Piyasin⁴, Apichart Boonma^{5,*}

Abstract: Mandibular reconstruction after tumor resection requires stable fixation that restores function and facial symmetry while minimizing invasiveness. This study presents and validates a bicortical screw-plate Temporary External Fixator (TEF) designed to enhance early-stage mandibular stabilization through optimized geometric configuration. An integrated approach combining finite element analysis (FEA) and experimental compression testing was employed to evaluate biomechanical performance under physiologically representative masticatory loads. Finite-element models of three TEF configurations (2-, 3-, and 4-screw) were analyzed using isotropic and anisotropic bone properties. Loads were applied as a static 600 N and a cyclic half-sine waveform. The 3-screw configuration exhibited the highest stiffness of 272.7 N/mm, lower peak cortical stress (26.49 MPa), and energy absorption of 0.96 J. The experimental tests on 3D-printed resin mandibles closely matched the FEA predictions, with displacement deviations below 5%, confirming the model's predictive reliability. The results highlighted that strategic screw placement and spacing had a larger impact on biomechanical performance than screw count alone. The proposed TEF demonstrated favorable structural efficiency, procedural simplicity, and cost-effectiveness. The computational-experimental framework established in this work supports future patient-specific optimization and fatigue-life studies for the development of next-generation external fixators in mandibular reconstruction.

Keywords: Biomechanical performance; Finite element analysis; Mandibular reconstruction; Screw-Plate system; Temporary external fixator

1. Introduction¹

Mandibular reconstruction after segmental defects from trauma, tumor resection, or congenital anomalies remains challenging because the mandible underpins speech, mastication, and facial esthetics; restoring both form and function is therefore critical (Sood et al., 2021). Although definitive reconstructive options have advanced, important limitations persist in the earliest postoperative phase when mechanical integrity is most vulnerable. Non-vascularized bone grafts show widely variable failure rates of 10%–54% in immediate reconstructions, and

¹Department of Mechanical and Manufacturing, Engineering, Faculty of Science and Engineering, Kasetsart University, Sakon Nakhon, 47000, Thailand

²Department of Civil and Environmental Engineering, Faculty of Science and Engineering, Kasetsart University, Sakon Nakhon, 47000, Thailand

³Dental Department, Sakon Nakhon Hospital, Sakon Nakhon, 47000, Thailand

⁴Department of Mechanical Engineering, Faculty of Engineering, Khon Kaen University, Khon Kaen, 40002, Thailand

⁵Department of Industrial Engineering, Faculty of Engineering, Khon Kaen University, Khon Kaen, 40002, Thailand

^{*}Corresponding author: apicbo@kku.ac.th; Tel.: +66-91-205-1157

¹For grants, please provide the grant number and the year it was received. Write it as follows: "This work was supported by the 'Name of organization' funded by 'Name of Grant and number' "

even delayed reconstructions using microvascular free flaps can fail in a non-trivial fraction of cases (approximately 10%) (Alencar et al., 2018). Meta-analytic comparisons further emphasize the premium on robust fixation and complication avoidance, with success rates reported around 96% for microvascular free flaps versus 75.6% for non-vascularized grafts (Govoni et al., 2023). These outcomes underscore the need for improved, anatomy-compatible stabilization strategies that protect alignment and soft tissues during the early healing window and interface well with subsequent definitive reconstruction.

Temporary external fixators (TEFs) are commonly used to bridge this interval, align segments, preserve occlusion, and protect soft tissue until definitive reconstruction is feasible (Bobinskas et al., 2016; Chaiyachet et al., 2024). Historically, TEF frames evolved in parallel with rigid internal fixation, using combinations of transosseous pins, Kirschner wires, connecting rods, and adjustable joints to maintain segmental stability during early recovery (Pankaj, 2022). However, conventional TEF designs typically rely on Schanz screws inserted approximately perpendicular to the bone surface (Figure 1). This configuration interacts sub-optimally with the curved geometry and complex load paths of the mandible, thereby predisposing to implant loosening, localized bone damage, soft-tissue irritation, and suboptimal stability under functional loads (Jaber et al., 2023; Schönegg et al., 2022). However, patient-specific implants manufactured by 3D printing can address geometric conformity but often face high costs, long lead times, and workflow complexity that limit routine use (Y. Liu et al., 2024). Thus, optimizing screw-plate configurations within the TEF paradigm represents a practical path to improve biomechanical efficiency while retaining surgical simplicity and cost consciousness.

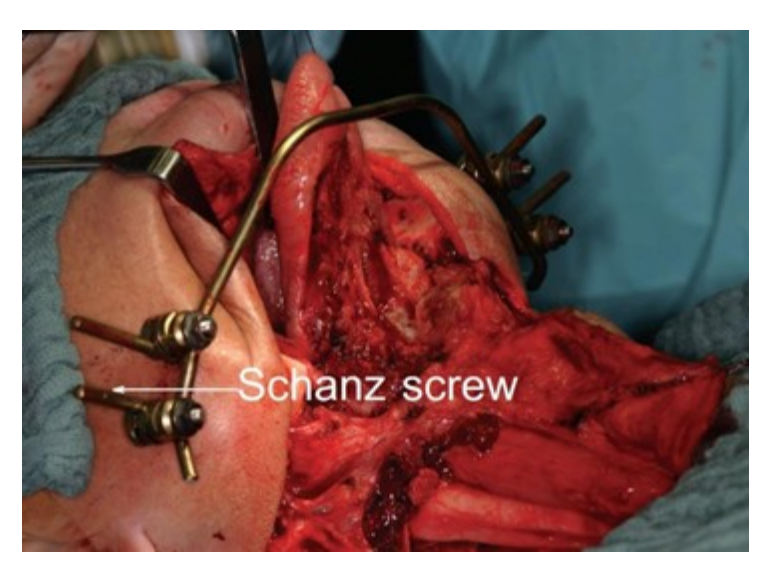


Figure 1 Intraoperative photograph of a conventional external mandibular fixation device with contoured connecting rods and Schanz screws. Adapted from Smolka et al., 2016, with permission from John Wiley & Sons, Ltd., The British Association of Oral Surgeons

Over the last decade, the research community has increasingly used computer-aided design and finite element analysis (FEA) to investigate and refine fixation strategies for the edentulous and dentate mandible. FEA enables systematic, in-silico comparisons of stress, strain, and displacement across alternative constructs, including modular architectures and bicortical screw configurations designed to distribute forces more evenly and reduce peri-implant stress concentrations (Bujtár et al., 2010; Chen et al., 2013; Chaiyachet et al., 2025; Izra'ai et al., 2025). However, important gaps remain. First, many studies emphasize static loading conditions—useful for bounding peak bite forces but insufficient to capture the time-dependent, multidirectional nature of mastication that alternates compression, torsion, and shear (Zhou et al., 2020). This limitation constrains insights into fatigue behavior, micromotion, and long-term stability (Ahmad Kholil, 2023; J. Wang et al., 2020). Second, paired experimental validation remains limited, and differences between resin or synthetic models and anisotropic living bone

can lead to discrepancies in absolute responses (M. C. Wang et al., 2023; Koper et al., 2021). The most robust investigations integrate FEA with mechanical testing to confirm trends and calibrate models, thereby improving the reliability and translational value of biomechanical inferences (Shi et al., 2021).

To address these needs, this study introduces and evaluates a bicortical screw-plate TEF concept intended to improve stability while better accommodating mandibular curvature and anatomic variability. The device is compatible with standard surgical instruments and aims to streamline intraoperative applications. To ensure numerical stability, reproducibility, and direct bench comparison, a representative bilateral static compressive load of 600 N was used. Although physiological loads are multidirectional and cyclic, these conditions were not modeled in the present work; rather, they motivated our design rationale and will be incorporated in future studies to broaden biomechanical assessment and strengthen translational relevance. We aim to generate cross-validated evidence about interface stresses, construct stiffness, and displacement patterns that can guide iterative TEF design and, ultimately, clinical application by combining FEA with mechanical testing on 3D-printed resin mandibles.

This study aims to quantify von Mises stress at the bone–screw interface of the bicortical screw–plate TEF under a representative bilateral static masticatory load of 600 N, evaluate construct stability by measuring structural stiffness and displacement at key mandibular land-marks, and validate biomechanical performance by comparing finite element analysis predictions with bench measurements on 3D-printed resin mandibles subjected to equivalent compressive loading. Taken together, these contributions advance TEF design toward structurally efficient, anatomy-adaptable, and potentially cost-conscious solutions. With further validation under cyclic, multidirectional loading and in anatomically faithful substrates, the findings may inform fixation strategies that reduce bone disruption, improve early-phase stability, and streamline surgical workflows in mandibular reconstruction.

2. Materials and Methods Used

Temporary external fixators (TEFs) in mandibular reconstruction provide interim stabilization for patients undergoing segmental mandibulectomy, particularly when access to 3D patient-specific modeling is limited. Although TEFs can theoretically achieve definitive bone healing, they are most often used as provisional stabilization before internal fixation because of practical stability constraints. Clinically, TEFs can maintain occlusion and facial contour and are especially useful for exophytic lesions involving the soft tissues of the cheek.

2.1 Conversion of Mandibular DICOM Data to 3D Printable STL Models

Computed tomography (CT) data in Digital Imaging and Communications in Medicine format were obtained from patients and processed to generate three-dimensional (3D) mandibular models. CT scans were performed using specific parameters to ensure high-resolution imaging, which is essential for precise modeling. DICOM files were imported into Mimics Research (Materialise., 2021) for detailed processing and segmentation. Because the mechanical tests used resin mandibles with uniform properties, a solid (homogeneous) bone model was created to mirror the test specimens.

The segmentation was accurately performed by thresholding Hounsfield units (HU) to isolate the mandibles, followed by slice-by-slice refinement using Mimics editors to correct residual artifacts and ensure anatomical fidelity. The segmented geometry was then wrapped and smoothed to yield a continuous, watertight surface suitable for downstream CAD/FEA steps (Ahmad et al., 2020). The final surface mesh was exported as a stereolithography (.STL) file and imported into SolidWorks for model assembly and fixture design (Dassault Systèmes., 2020).

2.2 TEF components and functionalities

A single segmental defect was modeled at the parasymphysis with a 10-mm gap to represent a typical reconstruction scenario (Chaiyachet et al., 2025). To replicate clinical placement, TEF components (plate and bicortical screws) were designed in SolidWorks and positioned on the mandibular segments. Inter-screw spacing on the mandible side was set at 12 mm, consistent with recommended titanium plate-hole spacing for bone fixation (Prasadh et al., 2022).

This spacing governs the local stress distribution, device stability, and load transfer between the mandible and fixator. Using realistic distances ensures that subsequent analyses reflect clinically relevant biomechanics. Screw-plate layouts comprising two, three, and four screws were prepared for comparison. Figure 2 illustrates the TEF components, materials, and anatomical positioning during tumor resection, providing a visual reference for the modeled clinical configuration.

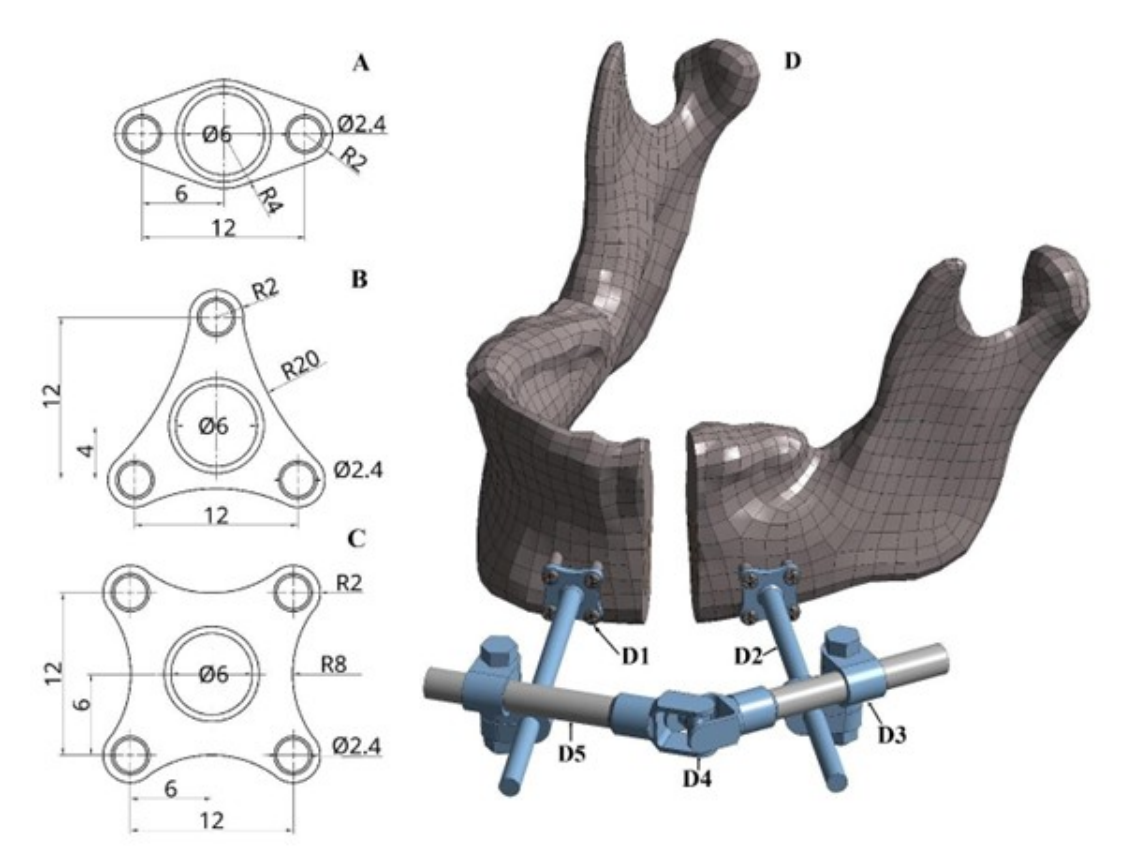


Figure 2 Screw-plate layouts and TEF assembly for mandibular fixation. (A) 2-screw plate, (B) 3-screw plate, (C) 4-screw plate, and (D) TEF mounted on a segmented mandible with labeled components: D1, bicortical screw (Ti-6Al-4V); D2, screw plate (SS316L); D3, clamp lock (SS316L); D4, connector joint (SS316L); and D5: external rod (carbon fiber)

2.3 Finite Element Analysis (FEA) Setup and Simulation Protocol

Finite element simulations were performed in ANSYS Workbench to evaluate the mechanical performance and structural response under representative loading (ANSYS Inc., 2021). The material properties for all components were compiled from experimental biomechanical data and literature sources and are summarized in Table 1 (Bazyar et al., 2023; Formlabs, 2024; MatWeb, 2024; Narra et al., 2013; Tümer et al., 2020). The mandible was modeled as a homogeneous, isotropic, linearly elastic solid to balance numerical accuracy with computational cost. This approach was consistent with assumptions commonly adopted in finite-element studies of skeletal fixation (Hemathulin et al., 2024; Zheng et al., 2022).

This representation is suitable for capturing global deformation patterns and overall stress

distributions under defined loads. However, it does not reproduce the anisotropic and heterogeneous characteristics of real bone. Simulations that are more physiologically realistic can incorporate direction-dependent properties to better reflect load transfer and local stress field, although with higher computational demands (Bazyar et al., 2023).

Materials	\mathbf{E}_1 GPa	\mathbf{E}_2 GPa	\mathbf{E}_3 GPa	$egin{array}{c} \mathbf{G}_{12} \ \mathbf{GPa} \end{array}$	$egin{array}{c} \mathbf{G}_{23} \ \mathbf{GPa} \end{array}$	$egin{array}{c} \mathbf{G}_{13} \ \ \ \ \ \ \ \ \ \ \ \ \ \ \ \ \ \ \$	$ u_{12}$	ν_{23}	ν_{13}	Yield Strength (MPa)
Ti-6Al-4V	114	114	114	-	-	-	0.34	-	-	880
316L SS	193	193	193	-	-	-	0.28	-	-	205
Resin	2.0	2.0	2.0	-	-	-	0.30	-	-	39
Carbon Fiber	350	350	350	-	-	-	0.30	-	-	2,231
Cortical Bone	16.0	6.3	6.3	3.2	3.6	3.3	0.30	0.30	0.45	-
Cancellous Bone	1.352	0.822	0.822	0.399	0.370	0.399	0.30	0.30	0.45	-

Table 1 Mechanical properties for the finite element analysis

The analyzed materials (Ti-6Al-4V, 316L stainless steel, resin, carbon fiber, cortical bone, and cancellous bone) were modeled as isotropic or orthotropic solids depending on their structural anisotropy. For orthotropic materials, three Young's moduli (E₁, E₂, E₃) represent stiffness along the longitudinal, transverse, and through-thickness axes, respectively; three shear moduli (G_{1 2}, G_{2 3}, G_{1 3}) describe the resistance to shear deformation on the 1–2, 2–3, and 1–3 planes, respectively; and three Poisson's ratios ($\nu_{1 2}$, $\nu_{2 3}$, $\nu_{1 3}$) define the transverse strain induced under uniaxial loading.

2.4 Meshing

2.4.1 Geometry Acquisition and Finite Element Model Setup

A 3D model of the external fixator assembly was created in SolidWorks 2023 and exported in STEP format for analysis. Finite element simulations were performed in ANSYS Workbench 2023 R1 using the Static Structural module. To accommodate geometrical complexity, the model was discretized with 10-node quadratic tetrahedral elements using an unstructured free meshing technique (Keddar et al., 2022).

2.4.2 Mesh convergence study

A mesh convergence study was conducted by systematically refining the element size and evaluating the maximum displacement at the point of load application to ensure the numerical reliability of the finite element analysis (FEA). The relative percent error in displacement, x between successive mesh refinements was calculated as Equation 1.

$$\varepsilon(x) = \left(\frac{|u_{x,i} - u_{x,i-1}|}{u_{x,i}}\right) \times 100\% \tag{1}$$

where $u_{x,i}$ denotes the displacement for mesh size i. $u_{x,i-1}$ is the displacement from the preceding (finer) mesh. Convergence was achieved when the percentage difference between refinements dropped below a threshold of 5%.

The mesh convergence study was conducted using systematically refined element sizes ranging from 1.2 to 0.2 mm. The total deformation values showed only minor variation as the mesh was refined, with the relative percent change progressively decreasing. At an element size of 0.8 mm, the maximum deformation was 89.917 μ m, and the change between successive refinements dropped below 0.1%. Further refinement to 0.2 mm resulted in negligible differences (<0.12%), confirming convergence of the solution. Therefore, the 0.8-mm mesh, which consisted of ap-

proximately 317,371 elements, was selected for all subsequent analyses as it provided adequate numerical accuracy while maintaining computational efficiency.

2.5 Boundary, loading, and contact conditions

The boundary, loading, and contact constraints were defined in the finite element model to replicate physiological and experimental conditions. To represent joint immobilization, the temporomandibular joints (TMJs) were fully constrained in all translational and rotational degrees of freedom, while the anterior teeth and mandibular base were fixed in translation to reproduce the experimental support setup. To simulate manual compression, a bilateral static load of 600 N was applied as uniform pressure along the inferior mandibular border (Gutwald et al., 2017). This magnitude was selected to reflect the physiological bite force range of healthy adults, thereby providing a realistic mechanical challenge without inducing nonphysiological failure. The load was prescribed as the surface pressure to avoid numerical singularities and to more accurately represent the cortical load transfer (Wilken et al., 2024).

A cyclic load of 600 N was applied in the transient structural analysis to capture dynamic masticatory behavior using a half-sine waveform at a frequency of 1 Hz, corresponding to three chewing cycles over a total duration of 3 s (Jia et al., 2014). Each chewing cycle was modeled as a half-sine waveform applied over 0.5 s, followed by a 0.5-s unloading phase (duty ratio = 50%), defined mathematically as follows:

$$F(t) = \begin{cases} \text{Load} \cdot \sin\left(\frac{\pi(t - t_i)}{0.5}\right), & t_i \le t \le t_i + 0.5, \\ F(t) = 0, & \text{otherwise.} \end{cases}$$
 (2)

Contact interactions were defined to reflect clinical mechanics: a friction coefficient of 0.3 was applied at screw-bone interfaces to simulate sliding resistance and potential loosening (Koper et al., 2021); bonded contacts were assigned at plate-screw-mandible interfaces to ensure rigid fixation (Lewis et al., 2021); and frictionless contact was specified at the defect site to allow controlled displacement while maintaining numerical stability (Sagl et al., 2019). Overall, these boundaries and loading conditions were selected to balance physiological realism with computational efficiency. Figure 3 shows the boundary conditions and loading configuration applied to the mandible model.

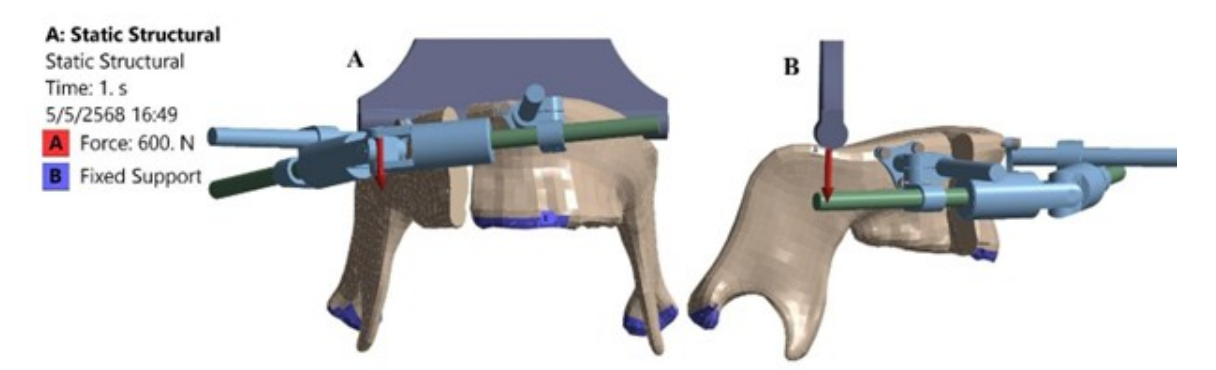


Figure 3 Boundary conditions and loading in the finite-element mandible model with TEF. (A) Static structural setup showing fixed supports at the condylar regions and the anterior teeth contact area (purple). (B) Vertical compressive load of 600 N applied via the loading indenter (red arrow)

2.6 Sensitivity analysis

A systematic sensitivity analysis was conducted to evaluate the robustness of the finite element model. Four key parameters were varied: (I) the screw spacing, adjusted by ± 3 mm

around the baseline 12.0 mm (9.0 and 15.0 mm) to assess the influence of fixation geometry on load transfer; (II) the applied load, varied between 480 and 720 N ($\pm 20\%$ of the baseline 600 N) to represent physiological fluctuations in masticatory force; (III) the elastic modulus (E₁), modified from 12 to 20 GPa ($\pm 30\%$ of the baseline 16 GPa) to capture the material range from 3D-printed resin to cortical bone; and (IV) the mesh density, refined from 1.0 to 0.6 mm (baseline 0.8 mm) element size to evaluate discretization effects.

The sensitivity analysis quantified how variations in geometric, loading, material, and meshing parameters affect mandibular displacement and stress responses, thereby establishing the model's numerical stability and reliability.

2.7 Finite element analysis validation through experimental testing

Experimental validation of the finite element model was experimentally validated using 3D-printed resin mandible models fabricated via LFS with a Form3 printer (Formlabs, 2024) using White Resin V4. These models replicated the human mandible's anatomical and structural features. A 10-mm-wide discontinuity was incorporated at the mandibular angle to simulate a clinically representative segmental defect (Chaiyachet et al., 2025), aligning with cases that commonly require reconstruction using vascularized osteocutaneous free flaps, such as the fibula flap (Figure 4). TEF devices were mounted on the resin models using 2.4 mm × 18 mm bicortical screws inserted into predrilled holes and secured with screw plates.

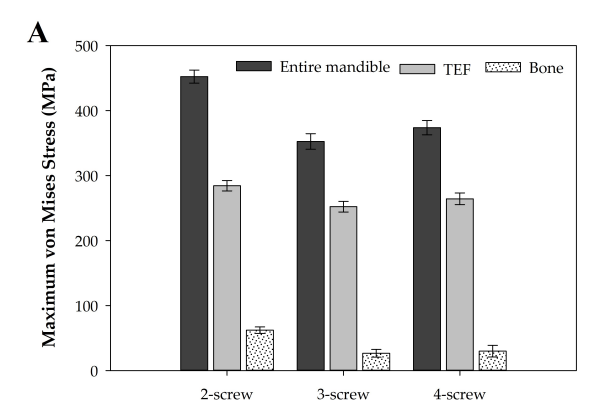
The assembled models were subjected to mechanical testing using an Instron Bionix® machine (MTS Insight, 100 kN) under a load-to-failure protocol. A 10 N preload was applied, followed by a compressive load at 1 N/s until failure, defined as mandible fracture, screw loosening, or displacement exceeding 20 mm (Koper et al., 2021). The resin mandible was rigidly clamped within a custom-designed jig to prevent unwanted motion during loading. A vertical compressive force was applied at the molar region using a loading indenter to replicate occlusal loading. The TEF system remained preassembled throughout testing to ensure that the fixation conditions were consistent with the FEA model.



Figure 4 Experimental compression testing of 3D-printed mandible resin models with TEF screw—plate configurations: (A) 2-screw, (B) 3-screw, and (C) 4-screw

3. Results and Discussion

FEA using isotropic material properties under a static 600 N load revealed that the 3-screw 2.4 mm bicortical configuration reduced peak von Mises stress within the mandible while maintaining structural integrity at the bone–fixator interface and within the overall TEF assembly. The maximum cortical stress decreased from 62.18 MPa in the 2-screw model to 26.49 MPa with three screws and 20.60 MPa with four screws, reflecting improved load sharing and fixation stability. The 3-screw configuration exhibited a more uniform stress distribution and greater mechanical efficiency, indicating that the number and spatial arrangement of screws influence the fixation performance. Figure 5 shows the corresponding FEA results for maximum von Mises stress and strain across the mandible, TEF construct, and peri-screw bone.



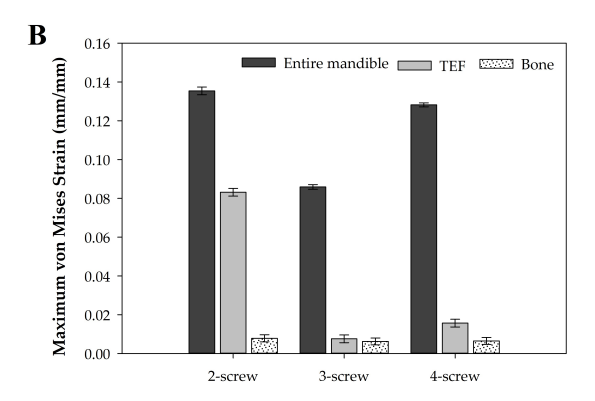


Figure 5 FEA-derived von Mises stress and strain across screw-plate configurations. (A) Maximum von Mises stress, and (B) Maximum von Mises strain for Entire Mandible, TEF and Bone surrounding screws

Under cyclic masticatory loading, a half-sine waveform with a peak force of 600 N applied across three chewing steps with 50 steps/cycle further corroborated these findings. To enhance physiological realism, the properties of anisotropic materials were assigned to both cortical and cancellous bone (Bazyar et al., 2023). The 3-screw fixation construct exhibited a peak deformation of 1.054 mm, maximum von Mises stress of 261.07 MPa, and strain of 0.019 mm/mm. In contrast, the 2-screw configuration showed greater deformation (1.276 mm) and higher stress (304.30 MPa) and strain (0.023 mm/mm), indicating increased local stress concentration. The 4-screw construct produced slightly lower deformation (1.165 mm) but elevated stress (302.34 MPa) and reduced strain (0.021 mm/mm), reflecting higher rigidity with intensified stress distribution. Overall, the 3-screw configuration provided the most balanced mechanical response, combining high stiffness with uniform load transfer and minimal cortical stress concentration. Under cyclic loading, the maximum cortical stress decreased markedly from 54.61 MPa in the 2-screw model to 27.69 MPa in the 3-screw configuration and 25.56 MPa in the 4-screw configuration (Figure 6).

These results indicate that reducing the number of screws increases local stress concentration and strain energy at the plate—bone interface, whereas adding screws enhances overall stiffness but may introduce overconstraint and elevated local stresses. The 2-screw configuration exhibited lower deformation but higher von Mises stress, indicating reduced stability under load. The 4-screw configuration produced slightly greater stiffness but concentrated stress near the fixation sites, reflecting diminished load-sharing efficiency. In contrast, the 3-screw configuration achieved a balanced mechanical response, combining moderate stiffness with uniform stress distribution across the mandible. Therefore, this configuration represents the most biomechanically efficient design, effectively mediating the trade-off between global rigidity and local stress concentration in screw fixation systems.

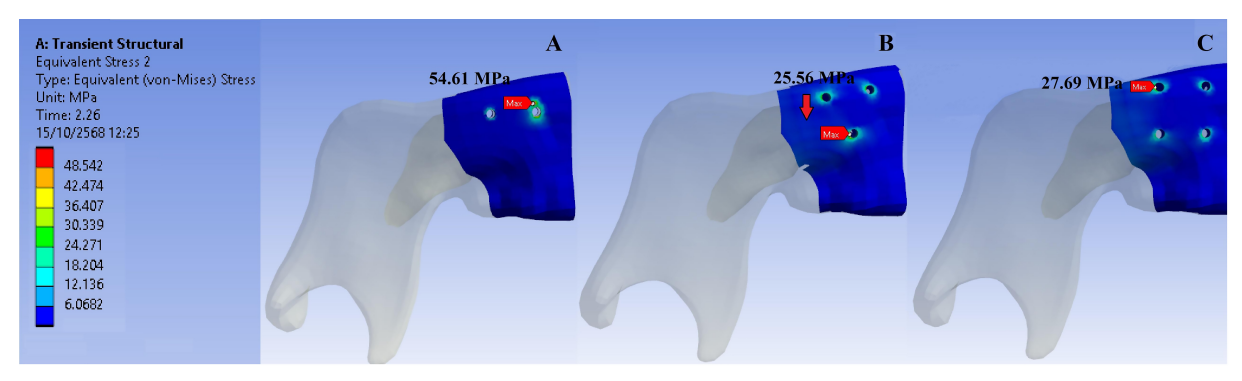


Figure 6 Maximum von Mises Stress on bone Distribution in 2-Screw, 3-Screw and 4-Screw

3.1 Results of Sensitivity Analysis

The sensitivity analysis demonstrated that the geometric, material, and numerical variations had minimal influence on the finite element predictions (Table 2). Varying the screw spacing by ± 3 mm from the baseline value of 12.0 mm resulted in a 10% change in displacement and a 13% change in peak cortical stress, indicating moderate geometric sensitivity. Load variations between 480 and 720 N ($\pm 20\%$) produced proportional increases in displacement (20.2%) and stress (22.6%), consistent with the physiological range of linear elastic behavior. In contrast, modifying the longitudinal elastic modulus (E₁) from 12 to 20 GPa affected displacement by less than 1% and stress by less than 0.5%, confirming low material sensitivity. Refining the mesh from 1.0 mm to 0.6 mm altered the displacement and stress by less than 1% and 5%, respectively.

Case ID	Parameter Change	Value	Peak von Mises stress (MPa)	Δ s.Baseline (%)	Peak Disp. (mm)	Δ s.Baseline (%)
BL	-	_	261.70	-	1.054	-
SS09	Screw spacing	9.0	312.10	19.25	1.003	-4.83
SS15	(mm)	15.0	294.59	12.56	0.953	-9.58
L480	Load (N)	480	281.95	7.73	0.816	-22.58
L720	Load (N)	720	254.71	-2.67	1.267	20.20
E-12	Young's modulus	12	263.39	0.12	1.058	0.38
E-20	$(E_i:GPa)$	20	262.30	0.25	1.046	-0.76
M1.0	Mesh Size (mm)	1.0	273.33	4.44	1.055	0.09
M0.6	Mesii Size (IIIII)	0.6	260.80	-0.34	1.064	0.95

Table 2 Summary of Sensitivity Analysis Results

The sensitivity analysis (Table 2) demonstrated that the geometric, loading, material, and numerical variations had a limited influence on the finite element predictions. Varying the screw spacing by ± 3 mm from the 12 mm baseline caused a change of up to 19% in the peak von Mises stress and less than 10% in the displacement, indicating moderate geometric sensitivity. Load changes between 480 N and 720 N produced nearly proportional displacement responses (-22% to +20%) and minor stress deviations (<8%), consistent with linear elastic behavior within the physiological range. Mesh refinement from 1.0 to 0.6 mm altered displacement by <1% and stress by $\pm 4.5\%$, demonstrating numerical convergence and supporting the selection of the 0.8-mm mesh as a practical balance between accuracy and computational cost. Variations in the elastic modulus (12–20 GPa) affected results by <1%, indicating numerical stability. The predicted magnitudes agree with reported values for mandibular fixation systems (Bazyar et al., 2023), supporting the physical plausibility of the model. Overall, the finite element framework is numerically stable and reliable for comparative and parametric analyses and may serve as a sound basis for further optimization and patient-specific modeling.

3.2 Biomechanical performance of the TEF configurations

Finite element analysis (FEA) and experimental testing were used to evaluate the mechanical performance of Temporary External Fixator (TEF) systems with 2-, 3-, and 4-screw configurations. As shown in Figure 9, the 3-screw setup consistently demonstrated the most favorable biomechanical characteristics, achieving the highest stiffness (272.7 N/mm) and energy absorption (0.96 J). This configuration outperformed the 4-screw (250.0 N/mm, 0.88 J) and

^{*}Note: Abbreviations — BL: baseline model. Parameter variations are defined as follows: SS09 and SS12 represent screw spacings of 9 mm and 15 mm, respectively; L480 and L720 correspond to applied loads of 480 N and 720 N; E-12 and E-20 denote longitudinal Young's modulus of 12 GPa and 20 GPa; and M1.0 and M0.6 indicate mesh element sizes of 1.0 mm and 0.6 mm, respectively.

2-screw (214.3 N/mm, 0.60 J) alternatives.

Load-to-failure tests on 3D-printed resin mandibles were performed to confirm the computational findings. The 3-screw configuration achieved the greatest load-bearing capacity (1899.74 N) and the least displacement (2.05 mm), while the 2-screw setup showed the lowest performance (1044.78 N, 3.25 mm). The 4-screw arrangement offered moderate stability but also indicated possible overconstraint due to redundant fixation points. These results emphasize that optimal screw placement enhances fixation more effectively than simply increasing the number of screws. The load–displacement curves in Figure 7 demonstrate strong agreement between the FEA and experimental results, reinforcing the computational model's reliability.

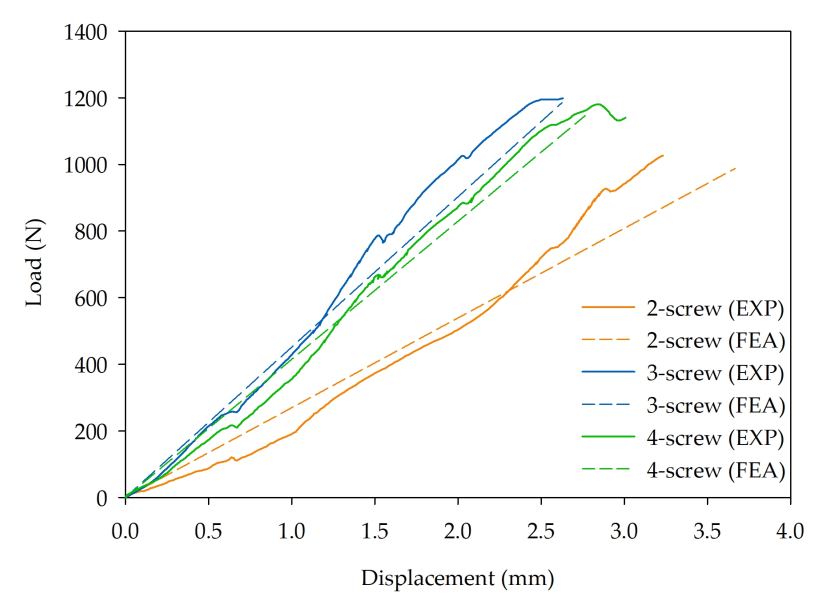


Figure 7 Comparison of Load–Displacement Curves from FEA and Experimental Testing of the TEF-Mandible Assembly

3.3 Compression Test Results and FEA Validation

FEA and compression testing showed the same performance ranking across all TEF configurations. The 3-screw layout consistently provided the greatest structural benefit, i.e., the highest stiffness and largest energy absorption, confirming its biomechanical advantage under the evaluated loading scenarios. The data are summarized in Table 3.

Table 3 Comparison of Stiffness and Energy Absorption Across TEF Configurations from FEA and Experimental Testing

	Stiffness	Stiffness		Energy	Energy	
Configuration	(N/mm)	(N/mm)	$\%\Delta$	Absorption	Absorption	$\%\Delta$
	FEA	Test		(J) FEA	(J) Test	
2-screw	214.3	368.4	-41.8%	0.6	0.445	+34.8%
3-screw	272.7	472.6	-42.3%	0.88	0.933	-5.7%
4-screw	250	468.6	-46.6%	0.6	0.794	-24.4%

Across configurations, FEA underpredicted stiffness by 41.8% - 46.6% relative to the experiment, whereas the energy absorption bias was configuration-dependent (-24.4% to +34.8%). These deviations are consistent with the idealized boundary conditions, linear-elastic material assumptions, and simplified contacts, which can depress absolute values while preserving relative

trends (Lewis et al., 2021). The trend agreement supports the use of this FEA framework for comparative assessment and early-stage design optimization.

Mechanistically, the 3-screw bicortical configuration likely improves force transmission and span triangulation across the defect, reducing local stress concentrations and distributing load more efficiently than either the 2-screw (insufficient constraint) or certain 4-screw layouts (added hardware not optimally placed relative to the neutral axis). This interpretation aligns with prior observations that screw configuration strongly shapes cortical and cancellous stress fields (Chaiyachet et al., 2025), as illustrated in Figure 8. Together, these results reinforce that optimized screw placement governs fixation performance and supports strategic, minimally invasive external-fixator designs rather than simply adding more hardware.

In context, conventional Schanz screw systems remain popular for their simplicity; however, they suffer from angular instability, loosening, and assembly complexity that can prolong surgery and compromise rigidity (Ellis III and Graham, 2002). Locking plates offer dependable internal stabilization but can cause peri-screw stress concentration and bone resorption under cyclic loading with predominantly monocortical engagement (Kano et al., 2007). Patient-specific implants (PSIs) achieve excellent anatomical conformity and load transfer but are limited by cost, lead time, and intraoperative inflexibility (Koper et al., 2021). The present findings place the proposed TEF as a practical middle ground, leveraging placement-optimized bicortical screws to approach the stability benefits of more complex constructs while maintaining procedural simplicity. Table 4 summarizes the key comparative features of TEF versus Schanz, locking plates, and PSIs. The proposed TEF integrates bicortical screw purchase with a modular, externally applied frame to improve fixation stability while streamlining the setup. Based on the present biomechanical data, it may function as a practical intermediate option between conventional systems and patient-specific implants, pending further clinical validation.

Table 4 Comparative design characteristics of mandibular fixation systems

Feature	Schanz screw	Locking plate	Patient-specific implant (PSI)	TEF (proposed)	
Fixation type	External	Internal	Custom internal	External	
Cortical purchase	Monocortical	Mostly monocortical	Monocortical or bicortical (design-dependent)	Bicortical	
Stability (general)	Moderate; risk of loosening	High; may concentrate stress	Excellent; precise fit	Improved; more uniform stress distribution	
Angular stability	Limited	Good (locking mechanism)	Excellent (custom geometry)	Good (screw-plate triangulation)	
Surgical complexity	Multi-step manual setup	Plate contouring and adaptation	Planning + fabrication; complex	Simple; modular assembly	
Customization	Standard parts	Limited	Fully customized	Semi-custom; adjustable	
Intraoperative flexibility	High	Moderate	Limited	High	
Manufacturing cost	Low		Very high	Low-moderate	
Typical clinical pin/screw loosening; lower rigidity		Peri-screw stress concentration; contouring time	Cost; lead time; limited intra-op changes	Under evaluation; promising	

Note: Characteristics of the Schanz screw, locking plate, and PSI were summarized from Ganser et al., 2007, K. Liu et al., 2021, Suojanen et al., 2017, and Michael et al., 2022. TEF characteristics were

obtained from this study.

The proposed bicortical screw—plate TEF combines the load-sharing benefits of bicortical purchase with the workflow efficiency of modular external systems. Under the static and cyclic masticatory loads defined in Section 3.5, finite element analysis indicated that the 3-screw TEF configuration yielded lower von Mises stress and smaller displacements than comparison constructs modeled within the same framework (Figure 6). Overall, the design offers a balanced solution among strength, simplicity, and affordability, with the potential to reduce operative time, hardware costs, and fixation-related complications as validation expands.

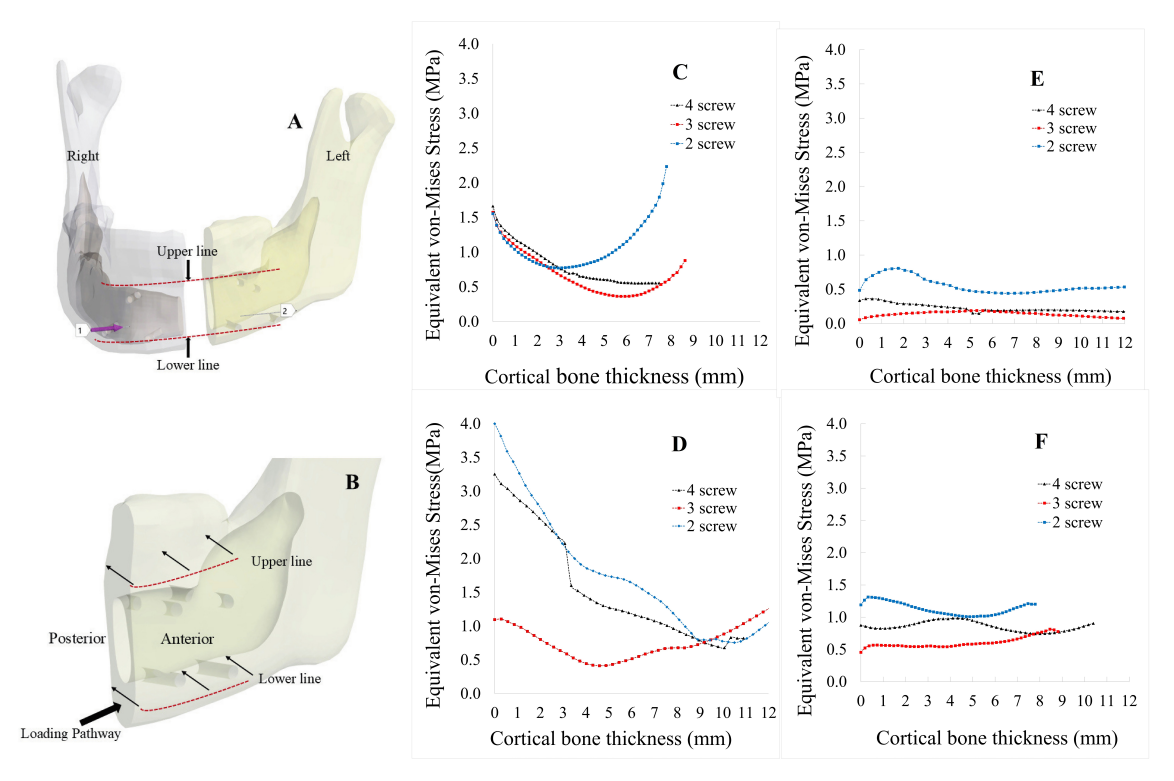


Figure 8 Von Mises (equivalent) stress in cortical bone across screw-plate configurations. (A) Finite-element model showing screw-plate placement on the mandibular segments. (B) Load application and boundary conditions used in the simulation. (C-F) Von Mises stress distributions sampled along the superior ("upper") and inferior ("lower") cortical tracks on the right (C, E) and left (D, F) hemimandibles. Adapted from Chaiyachet et al., 2025

The observed reduction in maximum equivalent von Mises stress within the cortical bone for the 3-screw plate configuration underscores its biomechanical efficiency in promoting uniform load transfer and mitigating localized stress concentrations. This stress reduction, consistently observed on both the right and left mandible regions across the upper and lower segments, suggests that screw quantity alone is not the primary determinant of fixation stability; rather, strategic placement plays a more influential role. These findings are consistent with those of previous research on the biomechanical behavior of screw fixation in mandibular reconstruction, particularly studies involving resorbable screws and their effects on stress distribution in in vitro models.

4. Conclusions

This study validated a bicortical screw-plate temporary external fixator (TEF) for mandibular reconstruction using an integrated FEA-experimental workflow. The three-screw configuration demonstrated superior mechanical performance, exhibiting an approximately 27% increase in stiffness and 47-110% improvement in energy absorption compared with the two-screw con-

figuration. It also provided more favorable load sharing and reduced peak von Mises stresses, indicating that strategic triangulation is more critical to mechanical performance than simply increasing hardware quantity. Although the linear elastic FEA model underestimated absolute stiffness values, it accurately ranked the relative performance across all configurations, supporting the utility of the integrated workflow for comparative screening. Limitations of the present study include the use of static loading conditions and isotropic material assumptions. Future work should incorporate anisotropic bone properties, nonlinear contact mechanics (including screw preload and frictional contacts in order to capture microslip and potential loosening), cyclic physiological loading to evaluate long-term fatigue resistance, and harmonized load applications and boundary conditions between experiments and simulations. Ultimately, the three-screw TEF offers a mechanically efficient and cost-effective solution for minimally invasive mandibular stabilization.

Acknowledgements

The authors would like to express their sincere gratitude to the Department of Mechanical and Manufacturing Engineering, Faculty of Science and Engineering, Kasetsart University; the National Science and Technology Development Agency, (NSTDA), Royal Thai Government; the Department of Industrial Engineering and the Department of Mechanical Engineering, Faculty of Engineering, Khon Kaen University; and the Dental Department, Sakon Nakhon Hospital, for their invaluable support and collaboration throughout this research.

Author Contributions

Rungsan Chaiyachet: Writing – Original Draft, Conceptualization, Methodology, Supervision. Weerayut Jina: Methodology. Ekkachai Kanchanatip: Writing – Review & Editing. Teerawat Paipongna: Conceptualization. Surasith Piyasin: Conceptualization, Software. Apichart Boonma: Conceptualization, Methodology, Supervision. All authors have read and approved the final manuscript.

Conflict of Interest

The authors declare no conflicts of interest. All authors confirm that there are no personal or financial relationships that could be perceived as influencing the interpretation or presentation of the research findings.

References

- Ahmad, M., Zulkifli, N., Shuib, S., Sulaiman, S., & Abdullah, H. (2020). Finite Element Analysis of Proximal Cement Fixation in Total Hip Arthroplasty. *International Journal of Technology*, 11, 1046. https://doi.org/10.14716/ijtech.v11i5.4318
- Ahmad Kholil, G. K. A. A. F. J. I. (2023). Finite Element Analysis of Lattice Structure Model with Control Volume Manufactured Using Additive Manufacturing. *International Journal of Technology*, 14(7), 291–319. https://doi.org/10.14716/ijtech.v14i7.6660
- Alencar, M. G. M. d., Bortoli, M. M. D., Silva, T. C. G. d., Silva, E. D. d. O. e., & Laureano Filho, J. R. (2018). Suitability of Wrist External Fixator for Treatment of Mandibular Fracture. *Journal of Craniofacial Surgery*, 29(4), e371–e372. https://doi.org/10.1097/scs.0000000000004375
- ANSYS Inc. (2021). ANSYS Workbench (Computer software; Version 21.0).
- Bazyar, P., Baumgart, A., Altenbach, H., & Usbeck, A. (2023). An Overview of Selected Material Properties in Finite Element Modeling of the Human Femur. *Biomechanics*, 3(1), 124–135. https://doi.org/10.3390/biomechanics3010012
- Bobinskas, A. M., Subramaniam, S. S., Vujcich, N. J., & Nastri, A. L. (2016). Bilateral distraction osteogenesis of vascularized iliac crest free flaps used in mandibular reconstruction.

- Plastic and Reconstructive Surgery-Global Open, 4(3), e635. https://doi.org/10.1097/GOX.00000000000000623
- Bujtár, P., Sándor, G. K., Bojtos, A., Szűcs, A., & Barabás, J. (2010). Finite element analysis of the human mandible at 3 different stages of life. *Oral Surgery, Oral Medicine, Oral Pathology, Oral Radiology, and Endodontology, 110*(3), 301–309. https://doi.org/10.1016/j.tripleo.2010.01.025
- Chaiyachet, R., Boonma, A., & Paipongna, T. (2024). Developing A Temporary External Fixator (TEF) For Mandibular Reconstruction Using Two-Phase QFD And TRIZ Approach. Sains Malaysiana, 53(5), 1201–1218. https://doi.org/10.17576/jsm-2024-5305-17
- Chaiyachet, R., Piyasin, S., Jina, W., Paipongna, T., & Boonma, A. (2025). Finite Element Analysis of a Novel Temporary External Fixator (TEF) in Mandibular Reconstruction. Journal of Applied Science and Engineering, 28(11), 2113–2125. https://doi.org/10.6180/jase.202511_28(11).0003
- Chen, A. C.-Y., Lin, Y.-H., Kuo, H.-N., Yu, T.-C., Sun, M.-T., & Lin, C.-L. (2013). Design optimisation and experimental evaluation of dorsal double plating fixation for distal radius fracture. *Injury*, 44(4), 527–534. https://doi.org/10.1016/j.injury.2012.09.022
- Dassault Systèmes. (2020). Solid Works (Computer software; Version 2020).
- Ellis III, E., & Graham, J. (2002). Use of a 2.0-mm locking plate/screw system for mandibular fracture surgery. *Journal of oral and maxillofacial surgery*, 60(6), 642–645. https://doi.org/10.1053/joms.2002.33110
- Formlabs. (2024). White Resin V4 (FLGPWH04) Technical Data Sheet [Retrieved May 20]. https://formlabs.com/materials/engineering/white-resin/
- Ganser, A., Thompson, R. E., Tami, I., Neuhoff, D., Steiner, A., & Ito, K. (2007). An in Vivo Experimental Comparison of Stainless Steel and Titanium Schanz Screws for External Fixation. European Journal of Trauma and Emergency Surgery, 33(1), 59–68. https://doi.org/10.1007/s00068-007-6053-5
- Govoni, F. A., Felici, N., Ornelli, M., Marcelli, V. A., Migliano, E., Pesucci, B. A., & Pistilli, R. (2023). Total mandible and bilateral TMJ reconstruction combining a customized jaw implant with a free fibular flap: a case report and literature review. *Maxillofacial Plastic and Reconstructive Surgery*, 45(1), 6. https://doi.org/10.1186/s40902-023-00374-w
- Gutwald, R., Jaeger, R., & Lambers, F. M. (2017). Customized mandibular reconstruction plates improve mechanical performance in a mandibular reconstruction model. *Computer methods in biomechanics and biomedical engineering*, 20(4), 426–435. https://doi.org/10.1080/10255842.2016.1240788
- Hemathulin, S., Nualsing, D., Pannucharoenwong, N., Nabudda, K., Paholpak, P., Echaroj, S., & Kongthip, P. (2024). Comparison of Treatment Positions for Tibia Fractures using the External Narrow Locking Compression Plate: 3D Finite Element Analysis. *Engineered Science*. https://doi.org/10.30919/es1300
- Izra'ai, S. I., Abdullah, A. H., Saari, A. B., Kasim, H. A., Hazwani, F., & Marwan, S. H. (2025). Computational Evaluation of Dental Adhesive for Four Direct Restorative Procedures. *International Journal of Online & Biomedical Engineering*, 21(3), 183–190. https://doi.org/10.3991/ijoe.v21i03.54099
- Jaber, M., Abouseif, N., Ibrahim, N., Hassan, M., & El-Ameen, A. M. (2023). Reasons for removal of miniplates used in fixation of maxillofacial bone fractures: systematic review and meta-analysis. *Applied Sciences*, 13(21), 11899. https://doi.org/10.3390/app132111899
- Jia, Y.-F., Xuan, F.-Z., Chen, X., & Yang, F. (2014). Finite element analysis of the cyclic indentation of bilayer enamel. *Journal of Physics D: Applied Physics*, 47, 175401. https://doi.org/10.1088/0022-3727/47/17/175401
- Kano, S. C., Binon, P. P., Bonfante, G., & Curtis, D. A. (2007). The effect of casting procedures on rotational misfit in castable abutments. *International Journal of Oral & Maxillofacial Implants*, 22(4).

- Keddar, I., Aour, B., & Zahaf, S. (2022). Comparative Study of the Fractured Humerus Fixation by Intramedullary Nailing and Compression Plate. *Journal of Failure Analysis and Prevention*, 22. https://doi.org/10.1007/s11668-022-01459-w
- Koper, D. C., Leung, C. A., Smeets, L. C., Laeven, P. F., Tuijthof, G. J., & Kessler, P. A. (2021). Topology optimization of a mandibular reconstruction plate and biomechanical validation. *Journal of the mechanical behavior of biomedical materials*, 113, 104157. https://doi.org/10.1016/j.jmbbm.2020.104157
- Lewis, G. S., Mischler, D., Wee, H., Reid, J. S., & Varga, P. (2021). Finite element analysis of fracture fixation. *Current osteoporosis reports*, 19(4), 403–416. https://doi.org/10.1007/s11914-021-00690-y
- Liu, K., Abulaiti, A., Liu, Y., Cai, F., Ren, P., & Yusufu, A. (2021). Risk factors of pin tract infection during bone transport using unilateral external fixator in the treatment of bone defects. *BMC Surgery*, 21(1), 377. https://doi.org/10.1186/s12893-021-01384-z
- Liu, Y., Wang, P., Telha, W., Jiang, N., Bi, R., & Zhu, S. (2024). Arthroscopic reduction and rigid fixation of the anteriorly displaced temporomandibular joint disc without reduction using titanium screw: a case series. *Clinical Oral Investigations*, 28(2), 156. https://doi.org/10.1007/s00784-024-05552-2
- Materialise. (2021). *Mimics Research* (Computer software; Version 21.0).
- MatWeb. (2024). Information on www.matweb.com [Retrieved May 20]. https://www.matweb.com
- Michael, L., Brian, S., Natalia von, W., Kyle, V., Nolan, S., & Matthew, O. (2022). Review of cost and surgical time implications using virtual patient specific planning and patient specific implants in midface reconstruction. *Plastic and Aesthetic Research*, 9, 26. https://doi.org/10.20517/2347-9264.2021.108
- Narra, N., Valášek, J., Hannula, M., Marcián, P., Sándor, G., Hyttinen, J., & Wolff, J. (2013). Finite element analysis of customized reconstruction plates for mandibular continuity defect therapy. *Journal of biomechanics*, 47. https://doi.org/10.1016/j.jbiomech.2013. 11.016
- Pankaj, P. (2022). Devices for traumatology: biomechanics and design. In *Human orthopaedic biomechanics* (pp. 459–484). Elsevier. https://doi.org/10.1016/B978-0-12-824481-4.00033-0
- Prasadh, S., Krishnan, A. V., Lim, C., Gupta, M., & Wong, R. (2022). Titanium versus magnesium plates for unilateral mandibular angle fracture fixation: Biomechanical evaluation using 3-dimensional finite element analysis. *Journal of Materials Research and Technology*, 18, 2064–2076. https://doi.org/10.1016/j.jmrt.2022.02.025
- Sagl, B., Schmid-Schwap, M., Piehslinger, E., Kundi, M., & Stavness, I. (2019). A dynamic jaw model with a finite-element temporomandibular joint. Frontiers in Physiology, 10, 1156. https://doi.org/10.3389/fphys.2019.01156
- Schönegg, D., Müller, G. T., Blumer, M., Essig, H., & Wagner, M. E. (2022). Two-versus three-screw osteosynthesis of the mandibular condylar head: a finite element analysis. *Journal of the mechanical behavior of biomedical materials*, 127, 105077. https://doi.org/10.1016/j.jmbbm.2022.105077
- Shi, Q., Sun, Y., Yang, S., Van Dessel, J., Lübbers, H.-T., Zhong, S., Gu, Y., Bila, M., Dormaar, T., & Schoenaers, J. (2021). Failure analysis of an in-vivo fractured patient-specific Ti6Al4V mandible reconstruction plate fabricated by selective laser melting. *Engineering Failure Analysis*, 124, 105353. https://doi.org/10.1016/j.engfailanal.2021.105353
- Smolka, W., Cornelius, C.-P., & Mast, G. (2016). Survival rates after surgical salvage procedures using mandible external pin fixation. *Oral Surgery*, 9(1), 19–24. https://doi.org/10.1111/ors.12163
- Sood, R., Ramu, J., Thankappan, K., & Iyer, S. (2021). Reconstruction of the Mandible and Choice of Flap. In *Management of oral cancers* (pp. 195–210). Springer. https://doi.org/ 10.1007/978-981-15-6499-4 15

- Suojanen, J., Leikola, J., & Stoor, P. (2017). The use of patient-specific implants in orthognathic surgery: A series of 30 mandible sagittal split osteotomy patients. *Journal of Cranio-Maxillofacial Surgery*, 45(6), 990–994. https://doi.org/10.1016/j.jcms.2017.02.021
- Tümer, D., Güngörürler, M., Havıtçıoğlu, H., & Arman, Y. (2020). Investigation of effective coating of the Ti–6Al–4V alloy and 316L stainless steel with graphene or carbon nanotubes with finite element methods. *Journal of Materials Research and Technology*, 9(6), 15880–15893. https://doi.org/10.1016/j.jmrt.2020.11.052
- Wang, J., Rai, R., & Armstrong, J. N. (2020). Investigation of compressive deformation behaviors of cubic periodic cellular structural cubes through 3D printed parts and FE simulations. Rapid Prototyping Journal, 26(3), 459–472. https://doi.org/10.1108/RPJ-03-2019-0069
- Wang, M. C., Kiapour, A., Massaad, E., Shin, J. H., & Yoganandan, N. (2023). A guide to finite element analysis models of the spine for clinicians. *Journal of Neurosurgery: Spine*, 40(1), 38–44. https://doi.org/10.3171/2023.7.SPINE23164
- Wilken, A., Schultz, J., Luo, Z.-X., & Ross, C. (2024). A new biomechanical model of the mammal jaw based on load path analysis. *The Journal of experimental biology*, 227. https://doi.org/10.1242/jeb.247030
- Zheng, F., Yunfan, Z., Gong, Y., Yin, D., & Liu, Y. (2022). Variation in stress distribution modified by mandibular material property: a 3D finite element analysis. *Computer Methods and Programs in Biomedicine*, 229, 107310. https://doi.org/10.1016/j.cmpb.2022.107310
- Zhou, F., Yang, S., Liu, J., Lu, J., Shang, D., Chen, C., Wang, H., & Ma, J. (2020). Finite element analysis comparing short-segment instrumentation with conventional pedicle screws and the Schanz pedicle screw in lumbar 1 fractures. *Neurosurgical Review*, 43, 301–312. https://doi.org/10.1007/s10143-019-01146-9